

Cross-species Transcriptomes Reveal Species-specific and Shared Molecular Adaptations for Plants Development on Iron-rich Rocky Outcrops Soils

Mariana Costa Dias

Universidade Federal de Minas Gerais

Cecílio Caldeira

Instituto Tecnológico Vale

Markus Gastauer

Instituto Tecnológico Vale

Silvio Ramos

Instituto Tecnológico Vale

Guilherme Oliveira (✉ guilherme.oliveira@itv.org)

Instituto Tecnológico Vale

Research Article

Keywords: Ironstone outcrops, Leguminosae, Caesalpinioideae, de novo transcriptome, gene expression plasticity, RNA-seq, comparative transcriptomics, Canga, Fabaceae

Posted Date: October 11th, 2021

DOI: <https://doi.org/10.21203/rs.3.rs-929174/v1>

License:   This work is licensed under a Creative Commons Attribution 4.0 International License.

[Read Full License](#)

Version of Record: A version of this preprint was published at BMC Genomics on April 19th, 2022. See the published version at <https://doi.org/10.1186/s12864-022-08449-0>.

Abstract

Background

Canga is the Brazilian term for the savanna-like vegetation harboring several endemic species on iron-rich rocky outcrops, usually considered for mining activities. *Parkia platycephala* Benth. and *Stryphnodendron pulcherrimum* (Willd.) Hochr. naturally occur in the *cangas* of Serra dos Carajás (eastern Amazonia, Brazil) and the surrounding forest, indicating high phenotypic plasticity. The morphological and physiological mechanisms of the plants' establishment in the *canga* environment are well studied, but the molecular adaptative responses are still unknown. We aimed to identify molecular mechanisms that allow the establishment of these plants in the *canga* environment.

Results

Plants were grown in *canga* and forest substrates collected in the Carajás Mineral Province. RNA was extracted from pooled leaf tissue, and RNA-seq paired-end reads were assembled into representative transcriptomes for *P. platycephala* and *S. pulcherrimum* containing 31,728 and 31,311 primary transcripts, respectively. We identified both species-specific and core molecular responses in plants grown in the *canga* substrate using differential expression analyses. In the species-specific analysis, we identified 1,112 and 838 differentially expressed genes for *P. platycephala* and *S. pulcherrimum*, respectively. Enrichment analyses showed unique biological processes and metabolic pathways affected for each species. Comparative differential expression analysis was based on shared single-copy orthologs. The overall pattern of ortholog expression was species-specific. Even so, almost 300 altered genes were identified between plants in *canga* and forest substrates, responding the same way in both species. The genes were functionally associated with the response to light stimulus and the circadian rhythm pathway.

Conclusions

Plants possess species-specific adaptative responses to cope with the substrates. Our results also suggest that plants adapted to both *canga* and forest environments can adjust the circadian rhythm in a substrate-dependent manner. The circadian clock gene modulation might be a central mechanism regulating the plants' development in the *canga* substrate in the studied legume species. The mechanism may be shared as a common mechanism to abiotic stress compensation in other native species.

Background

Outcrops of banded iron formations found in the Serra dos Carajás (Pará, Northern Brazil) typically occur in iron-rich areas worldwide¹. They are covered by diverse, savanna-like vegetation known in Brazil as *canga* that harbors many endemic species. These challenging environments are characterized by high temperatures and UV radiation, together with a strong seasonal water regime, shallow and acidic soils,

with low nutrients availability (especially phosphorus, magnesium, and calcium), and high total metal concentrations (such as iron and manganese)^{2, 3, 4}.

The *cangas* of Serra dos Carajás are inserted in the Amazon Rainforest, rising abruptly from the surrounding lowland vegetation matrix. Plant species of ironstone outcrops grow in high-stress habitats that restrict the species composition, resulting in structurally and floristically distinct vegetation from the surrounding forest, with many species unique to the *canga* environment⁵. Nevertheless, some species occur in both ecosystems, tolerating a wide range of conditions and displaying high phenotypic plasticity.

The main characteristics of plants adapted to the *canga* environment involve thick, waxy, coriaceous, and hairy leaves, protected stomata and stomata activity control, idioblasts containing phenolic compounds and crystals, and the presence of water-storing parenchymatous tissues, among other features^{2, 3, 6}. The *canga* plant community also presents metal tolerance by excluding or accumulating (or hyper-accumulating) metals in their shoots. Metal accumulation was recorded in several savanna species in the *cangas* of Carajás⁷. To our knowledge, there is no molecular study of the traits that allow *canga* plants to thrive in such a stressful environment.

Fabaceae, also known as Leguminosae, is one of the most prominent plant families found in the Carajás *cangas*, containing almost 80 species⁸. The family includes approximately 19,500 species under six recently described subfamilies: Cercidoideae, Detarioideae, Dialioideae, Duparquetioideae, Papilionoideae, and Caesalpinioideae, which contains the former subfamily Mimosoideae⁹. The most prominent ecological trait of the family is the possibility of some legume species to fix efficiently atmospheric nitrogen in symbiosis with soil bacteria¹⁰. This ability is an advantageous adaptation to occupy environments that are poor in nutrients, such as the *cangas*. Fabaceae comprises several socioeconomic crops, being the second most cultivated plant family¹¹.

Parkia platycephala Benth. and *Stryphnodendron pulcherrimum* (Willd.) Hochr. are two species of tropical Caesalpinioideae with distribution ranges comprising different bioclimatic regions, biomes, and habitats, with natural occurrences in *canga* environments (shrublands and woodlands) and surrounding forests. *P. platycephala* is endemic to Brazil, occurring in the domains of Amazon, Caatinga, and Cerrado¹², while *S. pulcherrimum* is more widely distributed over the South American continent, covering large phytogeographic domains of Amazon, Caatinga, and Atlantic Forest¹². Both species are suitable for mine land rehabilitation programs^{13, 14, 15, 16}, exhibiting fast growth rates and the capacity to tolerate drought^{14, 17}.

Because of their wide distribution and occurrence in forest and *canga* ecosystems from the Carajás region, both species were selected as models to study the phenotypic variation in the initial growth influenced by substrates from these contrasting environments¹⁴. In that study, the authors found that plants grown in unfertilized *canga* and forest substrates showed no difference in the initial growth rate. However, plants grown in the *canga* substrate showed higher foliar concentrations of Manganese (Mn)

and iron (Fe) and higher relative investment in root development¹⁴. Between the two species, only *S. pulcherrimum* exhibited symbiotic interactions with nitrogen-fixing bacteria, with a higher percentage when grown in the forest topsoil.

Environment-induced phenotypic plasticity plays an important role in organisms' development, function, and adaptation. Identifying natural genetic resources and characterizing adaptive genetic variation in *canga* plants may increase our knowledge of the genes linked to several abiotic stress such as heavy metals, nutrient deficiency, drought, and heat. This knowledge can be applied to native species in land rehabilitation¹⁶ and provide indications of adaptative responses relevant to species of agriculture importance, improving food security for crops subjected to climate changes¹⁸.

We studied the molecular mechanisms of adaptation to the *canga* soil compared to the forest, using two Leguminosae species, *P. platycephala* and *S. pulcherrimum*. The results indicated a species-specific adaptative responses and a core gene set responsive to the *canga* condition that may be shared by other plant species.

Results

The leguminous species were cultivated in *canga* and forest substrates collected at the Serra dos Carajás¹⁴. Plants grown in two trays of each substrate were harvested. Leaf samples from three individuals in the same tray were pooled together for RNA extraction. In the present study, we aimed to assemble high-quality and complete transcriptomes as references for *P. platycephala* and *S. pulcherrimum*. Furthermore, we sought to reveal the gene expression plasticity of the plants grown in substrates where they naturally occur and to establish if the species exhibit conserved molecular responses to *canga*. We used the well-established differential expression (DE) analyses to reveal the species-specific responses and orthologs DE analysis to test for conserved responses.

Transcriptome sequencing and de novo assembly

High-throughput RNA sequencing (RNA-seq) of leaf samples was used for the reference transcriptomes assembly. The sequencing output produced between 46–91 million paired-end reads per sample (See Supplementary Table S1, Additional File 1).

We used four *de novo* transcriptome assemblers to assemble the transcriptomes, implementing a range of k-mer sizes. Since each assembler and parameter set produces distinct sets of high-quality transcripts, several assemblies were generated to select the best set of recovered transcripts, as recommended by Gilbert (2013)¹⁹. In total, 15 assemblies were generated for *P. platycephala* and 17 for *S. pulcherrimum* (See Supplementary Table S2, Additional File 1), which were then merged into one over-assembly for each species. For both species, Trinity²⁰ produced assemblies with the highest average transcript length, highest N50 value, and highest number of assembled bases (See Supplementary Table S2, Additional File 1). SOAPDenovo-Trans²¹ had the longest transcripts (37,652 bp with k-mer size 61 for *P. platycephala*

and 49,517 bp with k-mer size 27 for *S. pulcherrimum*), but also the highest number of transcripts for both species. The number of contigs ranged from 121,698 and 94,733 with Velvet/Oases²² using a k-mer size of 61 to 255,644 and 233,410 with SOAPDenovo-Trans and a k-mer of 31 for *P. platycephala* and *S. pulcherrimum*, respectively (See Supplementary Table S2, Additional File 1).

The over-assembly approach enabled the recovery of many potential transcripts and their variants but resulted in very large assemblies containing many redundant sequences (Table 1). *P. platycephala* and *S. pulcherrimum* over-assemblies included 2,794,335 and 2,898,193 *de novo* assembled transcripts, respectively (See Supplementary Table S2, Additional File 1). The large assemblies were reduced with the EvidentialGene pipeline¹⁹. They resulted in 405,001, and 393,111 *de novo* assembled transcripts for *P. platycephala* and *S. pulcherrimum*, with 84,422 and 85,521 classified as the main set of transcripts (primary transcripts), respectively.

The Evigene draft transcript sets for *P. platycephala* and *S. pulcherrimum* are 7X above other Caesalpinioideae species set counts²³. Almost all the excess were unclassified short proteins. Of the main set, 28,561 (*P. platycephala*) and 27,632 (*S. pulcherrimum*) predicted proteins contained 120 amino acids (120aa) or more. According to Gilbert (2019)²⁴, most short putative proteins are spurious loci that can be discarded if no further classification evidence is established. Therefore, the main set's 55,861 and 57,889 short putative proteins were blasted (e-value 1×10^{-6}) against the UniProtKB/Swiss-Prot Viridiplantae database to attempt to establish homology evidence for them. Only 3,167 and 3,679 short proteins for *P. platycephala* and *S. pulcherrimum*, respectively, had hits with the Viridiplantae database and were kept for downstream analysis. The remaining short proteins and their alternative forms were discarded. From now on, primary transcripts with predicted proteins of 120aa or longer and the short ones with similarity to the Viridiplantae database will be referred to as the main filtered transcripts.

The differential expression (DE) analyses were performed with the samples from the *canga* and forest substrates to reveal the gene expression plasticity of the plants grown in substrates where they naturally occur. The main filtered transcripts added to their alternative forms were used for the species-specific DE analysis. The main filtered predicted proteins were used for orthology prediction. The single-copy orthologs were submitted to DE analysis between the substrates to test whether the species exhibit conserved molecular responses to the *canga* substrate.

Quality check and gene orthology prediction

The quality and completeness of the transcriptome can have a substantial impact on annotation and other downstream analyses. Errors in the transcriptome assembly could affect ortholog prediction, phylogenetic signal, and gene expression quantification^{25, 26}. We evaluated the rate of remapping and found that samples were aligned with their respective transcriptomes with mapping rates of 98.98% for *P. platycephala* and 99.19% for *S. pulcherrimum*.

To assess the completeness of the assemblies, we used the Benchmarking Universal Single-Copy Ortholog (BUSCO) assessment tool²⁷. The plant transcriptomes were compared against the embryophyta

and the eudicotyledons single-copy orthologs database. We achieved over 94% of the complete single-copy genes of embryophyta and eudicotyledons orthologs with BUSCO evaluation for both transcriptomes (Table 1). Many of these genes were duplicated in the assemblies, even after the EvidentialGene reduction, due to the presence of multiple isoforms. The BUSCO analysis with the main filtered transcripts (which excluded alternative isoforms) of the two species showed a marked decrease of the duplicated genes (from approximately 80–7% and 5%, for *P. platycephala* and *S. pulcherrimum*, respectively), maintaining at over 90% the recovery of complete orthologs of both embryophyta and eudicotyledons (Table 1). Additionally, only between 1.9% and 7.2% of near-universal genes were classified as missing in the plants' transcriptomes in all BUSCO analyses, indicating the transcriptomes' high quality and good coverage.

Table 1
BUSCO results from the de novo transcriptomes of *P. platycephala* and *S. pulcherrimum*.

| BUSCOs | <i>Parkia platycephala</i> | | | <i>Stryphnodendron pulcherrimum</i> | | |
|--|----------------------------|--------------------------|-------------------|-------------------------------------|--------------------------|-------------------|
| | Over-assembly | Evigene reduced assembly | Main filtered set | Over-assembly | Evigene reduced assembly | Main filtered set |
| Complete | 1358 (94.3%) | 1357 (94.3%) | 1314 (91.2%) | 1355 (94.1%) | 1354 (94.0%) | 1312 (91.1%) |
| | 2041 (96.2%) | 2046 (96.5%) | 2003 (94.5%) | 2027 (95.6%) | 2037 (96.0%) | 1981 (93.4%) |
| Complete and single-copy | 50 (3.5%) | 214 (14.9%) | 1201 (83.4%) | 34 (2.4%) | 205 (14.2%) | 1236 (85.8%) |
| | 70 (3.3%) | 311 (14.7%) | 1840 (86.8%) | 47 (2.2%) | 312 (14.7%) | 1862 (87.8%) |
| Complete and duplicated | 1308 (90.8%) | 1143 (79.4%) | 113 (7.8%) | 1321 (91.7%) | 1149 (79.8%) | 76 (5.3%) |
| | 1971 (92.9%) | 1735 (81.8%) | 163 (7.7%) | 1980 (93.4%) | 1725 (81.3%) | 119 (5.6%) |
| Fragmented | 28 (1.9%) | 28 (1.9%) | 44 (3.1%) | 22 (1.5%) | 21 (1.5%) | 24 (1.7%) |
| | 41 (1.9%) | 34 (1.6%) | 52 (2.5%) | 39 (1.8%) | 31 (1.5%) | 52 (2.5%) |
| Missing | 54 (3.8%) | 55 (3.8%) | 82 (5.7%) | 63 (4.4%) | 65 (4.5%) | 104 (7.2%) |
| | 39 (1.9%) | 41 (1.9%) | 66 (3.0%) | 55 (2.6%) | 53 (2.5%) | 88 (4.1%) |
| The <i>de novo</i> transcriptomes of <i>P. platycephala</i> and <i>S. pulcherrimum</i> were compared to the embryophyta (upper lines) and the eudicotyledons (bottom lines) databases. The percentage of inferred orthologs is in parentheses next to the number of orthologs. | | | | | | |

It is known that the quality of the transcriptome assembly affects phylogenetic inferences and that high-quality assemblies contribute to the greater consistency of established phylogenies²⁶. Thus, to further evaluate the transcriptome assemblies, we examined the molecular phylogeny of the recircumscribed Caesalpinioideae subfamily⁹. OrthoFinder²⁸ was used to detect putative orthologs and orthology grouping using the two transcriptomes' main filtered proteins and the predicted proteins of 16 genome or transcriptome sequences of other Caesalpinioideae species downloaded from multiple sources (See Supplementary Table S3, Additional File 1). The species tree was inferred from multiple sequence alignments generated with 331 single-copy orthogroups, with one sequence present in at least 14 (77.8%) of the 18 species analyzed. The tree was rooted with *Acrocarpus fraxinifolius* as an outgroup by the STRIDE algorithm²⁹. As expected, the ortholog phylogram shows the two species' placement within the Mimosoid clade and the relative proximity of each other (Figure 1a). Both species were part of a subclade composed of the genera *Inga*, *Albizia*, *Acacia*, and *Microlobius*. *P. platycephala* was the first species to diverge in this subclade, being sister to the remaining species. *S. pulcherrimum* was placed as a sister to *Microlobius foetidus*, as inferred from chloroplast and ITS data by Simon and collaborators (2016)³¹. The observed topology is supported by previous plastid-based studies, including the former Mimosoideae subfamily^{9,30,31,32}, and by the first effort for phylogenetic reconstruction using both plastid and nuclear data (transcriptome and whole-genome data) of the reclassified Fabaceae family¹¹. Therefore, our results confirm the close relatedness of both species, strengthen the phylogenetic consistency of the recircumscribed Caesalpinioideae subfamily, and the accuracy of the assembled transcriptomes.

To discover common expression patterns between *P. platycephala* and *S. pulcherrimum* during species development in the *canga*, we used the gene orthology information of both species inferred by OrthoFinder and compared the single-copy orthologs expression profiles. From the 63,039 queried predicted proteins of both species, a total of 53,763 were assigned to 16,958 orthogroups. 16,010 (94.4%) of the orthogroups were shared, 948 were classified as species-specific (Figure 1b), and 9,284 were single-copy for both species. The single-copy shared orthogroups were used for the conserved orthologs DE analysis.

Species-specific differential expression analysis under *canga* and forest substrates

We reduced the biological variability by pooling the leaf samples of three individuals grown in the same substrate for RNA extraction and sequenced two replicate pools for each condition³³. We also used stringent false discovery rate (FDR < 0.001, instead of the 0.05 usually found in RNA-seq studies) and \log_2 FoldChange thresholds ($|\log_2FC| \geq 2$) to reduce the number of false-positive differentially expressed genes (DEG) detected³⁴. Although this might increase the false-negative rates, it strengthens our confidence in the analyses.

To elucidate species-specific molecular mechanisms in response to the challenging *canga* environment, we identified differentially expressed genes in each species by comparing gene expression data in seedlings grown in forest substrate (control) to those grown in the *canga* substrate. The Spearman correlation coefficient of the expression values was calculated, showing higher correlations for the same condition than between conditions for both species (Figure 2). The DEGs were identified using the edgeR package³⁵. 1,112 and 838 DEGs (FDR <0.001) were determined for *P. platycephala* and *S. pulcherrimum*, respectively, including 390 up-regulated and 723 down-regulated genes for *P. platycephala* and 264 up-regulated and 574 down-regulated genes for *S. pulcherrimum* (See Supplementary Tables S4 and S5, Additional File 1). Both species had more down-regulated genes in plants grown in the *canga* substrate. However, the set of differentially expressed genes varied between species, indicating species-specific responses and adaptations.

To classify the DEGs' biological function, Gene Ontology (GO) enrichment analysis was carried out using Goseq³⁶. The GO enrichment analysis of the up-expressed genes identified 28 enriched terms (FDR < 0.05) for *P. platycephala* for the biological process (BP), cellular component (CC), and molecular function (MF) categories. For *S. pulcherrimum*, only the term "rhythmic process" was found enriched in the up-expressed genes. For the down-regulated genes, there were 85 (*P. platycephala*), and 131 (*S. pulcherrimum*) significantly enriched GO terms were detected for the BP, CC, and MF categories (See Supplementary Tables S6-S9, Additional File 1).

For *P. platycephala*, within the biological process category, the DEGs were mainly associated with 'response to light stimulus' and 'circadian rhythm' (Figure 3a). The GO terms 'rhythmic process', 'circadian rhythm', 'response to (abiotic, external, light, temperature) stimuli' were significantly enriched in up-regulated and down-regulated genes. However, the GO terms 'oxazole or thiazole biosynthetic process', 'polysaccharide catabolic process', and 'response to biotic stimulus' were enriched just in the up-regulated genes. The terms 'response to gibberellin' and 'photosynthesis' were enriched just in the down-regulated genes (See Supplementary Tables S6 and S7, Additional File 1). For *S. pulcherrimum*, 'rhythmic process' was the only enriched GO term in the up-regulated genes. The down-regulated genes were associated with the 'circadian rhythm', 'terpenoid catabolic process', 'response to (abiotic, light, radiation) stimuli and nutrient levels', and 'cellular response to phosphate starvation' (See Supplementary Tables S8 and S9, Additional File 1). Figure 3 shows the top 30 GO BP terms from the DEGs in *P. platycephala* (Figure 3a) and *S. pulcherrimum* (Figure 3b) grown in *canga* substrate. The complete list of enriched GO terms is in Supplementary Tables S6-S9, Additional File 1.

To further characterize the DEGs' function, a pathway-based analysis was performed using the KEGG pathway database (<https://www.genome.jp/kegg/>) with KOBAS³⁷. We identified 28 and 19 enriched (FDR < 0.05) pathways in *P. platycephala* and *S. pulcherrimum*, respectively, 15 of which are in common between the species. Figure 4 shows all the enriched KEGG pathways from the up- and down-regulated genes for both species. Exact FDR corrected *p*-values for each enriched pathway can be found in Supplementary Tables S10-S13, Additional File 1. The enriched pathways common to both species are related to the biosynthesis of secondary metabolites and their precursors in carbohydrate metabolism

and amino acid biosynthesis. Although both species showed similarly altered pathways, we also found some unique changed pathways. For *P. platycephala*, these pathways are related to the metabolism of cofactors and B-complex vitamins (porphyrin and chlorophyll; thiamine; vitamin B6; one carbon pool by folate), phenylpropanoid biosynthesis, photosynthesis, and peroxisome. For *S. pulcherrimum*, the exclusive pathways are related to lipid (glycerolipids; glycerophospholipids) and terpenoid metabolism.

Conserved orthologs differential expression analysis under *canga* and forest substrates

To facilitate the comparison of responses between the two species and observe the existence of genes altered in the same way in the initial development of the two species in the *canga*, we retrieved 9,284 single-copy orthologs. We investigated gene expression patterns across species and conditions with a hierarchical clustering analysis based on Spearman's correlation coefficient of gene expression between pairs of samples. Samples of the same species from different substrates clustered together, suggesting a general species-specific expression pattern of the orthologs (Figure 5a). The principal component analysis (PCA) also revealed the species-specific expression pattern, with the first component (PC1) separating the two species (Figure 5b). The two conditions (*canga* and forest) were separated along with the second component (PC2) (Figure 5b).

We then looked for orthologs that were differentially expressed in the same manner in the substrates for both plant species (Similarly responding differentially expressed orthologs - SRDEOs) to identify core genes involved in adapting to the *canga* substrate. We found 298 SRDEOs; 204 were up-regulated, and 94 were down-regulated (See Supplementary Table S14, Additional File 1). The direction of gene expression of detected SRDEOs was similar to that of the separate species analyses, with more down-regulated orthologs. Enrichment analysis identified 26 enriched GO terms (FDR < 0.05 - Table 2). Most terms were related to chloroplast, transcription regulation, circadian rhythm, and response to light stimulus. The enrichment analysis of the metabolic pathways showed only two enriched pathways (FDR < 0.05) in the SRDEOs: circadian rhythm and riboflavin metabolism. These results suggest that plants alter the expression of genes related to the perception of environmental variation depending on the substrate composition and that this effect may be related to the alteration of chloroplast functions. These genes, and the other orthologs similarly altered in the two species, may represent the molecular signature of these species in the *canga* environment.

Table 2
Gene Ontology terms identified as enriched by Fisher's exact test among SRDEOs.

| GO | Category | Term | FDR | Nº of genes |
|------------|----------|---|------------|-------------|
| GO:0009507 | CC | chloroplast | 1.51E-13 | 92 |
| GO:0006355 | BP | regulation of transcription, DNA-templated | 2.76E-08 | 39 |
| GO:0007623 | BP | circadian rhythm | 5.32E-08 | 12 |
| GO:0010114 | BP | response to red light | 2.69E-07 | 9 |
| GO:0005515 | MF | protein binding | 1.48E-06 | 60 |
| GO:0003700 | MF | DNA-binding transcription factor activity | 6.36E-06 | 36 |
| GO:0009649 | BP | entrainment of circadian clock | 1.64E-05 | 5 |
| GO:0010017 | BP | red or far-red light signaling pathway | 1.64E-05 | 6 |
| GO:0009535 | CC | chloroplast thylakoid membrane | 2.62E-05 | 14 |
| GO:0009570 | CC | chloroplast stroma | 3.02E-05 | 19 |
| GO:0009637 | BP | response to blue light | 0.00026005 | 6 |
| GO:0080167 | BP | response to karrikin | 0.00036018 | 8 |
| GO:0009416 | BP | response to light stimulus | 0.00053656 | 10 |
| GO:0009658 | BP | chloroplast organization | 0.00135533 | 8 |
| GO:0090351 | BP | seedling development | 0.00239464 | 4 |
| GO:0000427 | CC | plastid-encoded plastid RNA polymerase complex | 0.00340051 | 3 |
| GO:0032922 | BP | circadian regulation of gene expression | 0.00340051 | 3 |
| GO:0042752 | BP | regulation of circadian rhythm | 0.00563682 | 4 |
| GO:0042753 | BP | positive regulation of circadian rhythm | 0.006172 | 3 |
| GO:0010218 | BP | response to far red light | 0.01466872 | 4 |
| GO:0045892 | BP | negative regulation of transcription, DNA-templated | 0.01476035 | 7 |
| GO:0009909 | BP | regulation of flower development | 0.01476035 | 5 |
| GO:0009579 | CC | thylakoid | 0.02513588 | 7 |
| GO:0009654 | CC | photosystem II oxygen evolving complex | 0.02601454 | 3 |

BP – Biological Process; CC – Cellular component; MF – Molecular Function.

| GO | Category | Term | FDR | Nº of genes |
|--|----------|---|------------|-------------|
| GO:0009534 | CC | chloroplast thylakoid | 0.03019725 | 7 |
| GO:2000028 | BP | regulation of photoperiodism, flowering | 0.04020657 | 3 |
| BP – Biological Process; CC – Cellular component; MF – Molecular Function. | | | | |

Discussion

Canga plant communities are exposed to conditions that determine severe restrictions for their establishment. Especially restrictive are high metal concentrations, radiation, temperature, and low water storage capacity³. Molecular adaptative mechanisms of the native flora are largely unknown. The *P. platycephala* and *S. pulcherrimum* taxa are represented in the sequence databases with one chloroplast genome for each genus (*Parkia javanica* - Bioproject number: PRJNA390395 and *Stryphnodendron adstringens* - Bioproject number: PRJNA573224), and 16 DNA sequences from *P. platycephala* and 18 from *S. pulcherrimum* (Accessed on September 02, 2021). This work adds to the understanding of these species' molecular adaptative mechanisms and the description of their gene content. This is important not only for the region where industrial mining activities occur but also because the plants have a broad distribution to other regions. We used the assembled transcriptomes as references to investigate the plants' adaptative gene expression plasticity when grown in two naturally occurring substrates. We aimed at unraveling the molecular mechanisms implicated in abiotic stress compensation to the *canga* environment.

It is worth noting that, although the experiment was conducted in greenhouse conditions to diminish additional environmental variables, all substrates were collected in the field carried their original characteristics¹⁴. The goal was to understand the overall adaptative response to the different substrates and not identify the contribution of each variable individually. Studies investigating the gene expression responses to abiotic stimuli in multiple and concurrent stress conditions observe different transcriptomic patterns from those seen in highly controlled environments^{38, 39, 40, 41}. Thus, by maintaining the original substrates, we can get closer to the natural environments and better indicate the transcriptomic responses to the *canga* condition.

P. platycephala and *S. pulcherrimum* exhibited a similar direction of the altered transcriptional state, with more down-regulated than up-regulated genes, when grown in the *canga* substrate. The functional analysis indicated alterations in the metabolic pathways related to both species' primary and secondary metabolite synthesis. Approximately 52% and 75% of the altered pathways in *P. platycephala* and *S. pulcherrimum*, respectively, were shared between species, most related to primary metabolism, but with possible impact in secondary metabolites^{42, 43}. The pathways related to secondary metabolites differ in the two species, indicating that the species have different survival strategies. *P. platycephala* seems to direct the changes in gene expression mainly through the shikimate (shikimic acid) pathway, produced

from the glycolytic and pentose phosphate pathways (enriched in the analysis). This pathway produces phenylalanine, tyrosine, tryptophan (the last two enriched in the analysis), precursors of several secondary metabolites, including phenylpropanoids⁴³. *S. pulcherrimum* seems to direct the changes to the mevalonate pathway, which culminates in the production of lipids and terpenoids⁴³, over-represented in enrichment analyzes.

Phenylpropanoids are a group of secondary plant metabolites derived from phenylalanine that have various functions both as structural and signaling molecules. Thirteen over-expressed genes in *P. platycephala* in the *canga* soil were related to the phenylpropanoid biosynthesis, including the monolignol biosynthesis, the starting compounds for lignin biosynthesis, a key structural organic polymer for plant growth and development⁴⁴. Lignin confers cell wall rigidity, providing structural support and acting as a barrier against pathogens, and can also be involved in mineral nutrition and the plant's response to various environmental stresses, such as the tolerance of drought, heat, and heavy metals^{44, 45, 46, 47}, all observed in *canga* environment. Furthermore, it could also be acting as one of the physiological mechanisms involved in *P. platycephala* metal tolerance. Silva and collaborators¹⁴ previously observed high Zn and Mn availability in the substrate, together with elevated concentrations of Mn and Fe in the leaf tissues. Such lignin involvement in metal tolerance has also been reported for the Mn-hyperaccumulator *Phytolacca americana*⁴⁶. The sequestration of Mn into the leaf cell wall was also found to contribute to Mn tolerance in the sugarcane⁴⁸.

In addition, the up-regulated genes related to the phenylpropanoid biosynthesis pathway included peroxidase and cinnamyl-alcohol dehydrogenase, involved in the regulation of reactive oxygen species (ROS) levels⁴⁹. ROS can change the integrity of cell structure and lead to the denaturation of functional and structural proteins and lipid deterioration⁵⁰. Other *P. platycephala* altered pathways related to ROS regulation were peroxisome, ascorbate, alderate, and glutathione metabolisms. We observed DEGs coding for ROS scavenging enzymes, such as glutathione S-transferases, catalase (up-regulated), ascorbate peroxidase, and iron superoxide dismutase (down-regulated). The enzyme sarcosine oxidase produces glycine, formaldehyde, and hydrogen peroxide (H₂O₂) in peroxisomes, and was also found DE in *canga* plants.

P. platycephala exhibited down-regulation of genes related to photosynthesis and carbon fixation when cultivated in the *canga* soil. The downregulation of genes coding for photosynthetic proteins frequently has been observed in abiotic stresses, such as drought, salt, temperature, and heavy metals^{51, 52, 53}. High metal concentration in the photosynthetic tissue may reduce the synthesis of photosynthetic pigments and damage the photosynthetic machinery⁵⁴. The mechanisms adopted by the plants in this study are primarily related to the negative consequences on chlorophyll biosynthesis, the formation of the photosystems, and electron transport mechanisms. Genes related to the carbon fixation pathway were also down-regulated in *S. pulcherrimum* in *canga*. Despite the observed modulation in gene expression, a significant reduction in biomass accumulation or growth performance was not observed between the substrates¹⁴.

Genes involved in the terpenoid backbone biosynthesis were found down-regulated in *S. pulcherrimum*. Terpenoids are the largest class of secondary metabolites in plants and play essential roles in relieving abiotic and biotic stresses⁵⁵. The altered genes in this pathway code for enzymes that catalyzes reactions releasing pyrophosphate (Geranylgeranyl pyrophosphate synthase, Dehydrodolichyl diphosphate synthase complex, Solanesyl-diphosphate synthase 2, Geranylgeranyl diphosphate reductase). Phosphorus concentration was higher in the *canga* substrate¹⁴. Moreover, forest grown *S. pulcherrimum* showed lower leaf P content¹⁴. The up-regulation in terpenoid biosynthesis observed in plants grown in forest substrate may be related to the low P availability. Phosphorus influences terpenoid production since its synthesis depends on ATP and NADPH, and terpenoid precursors contain high-energy phosphate bonds^{56, 57}. Here we suggest that terpenoids may act as phosphate providers under P-limiting conditions.

Enrichment analyzes indicated a response of *S. pulcherrimum* to P deprivation in the forest substrate with 15 GDEs associated with the GO term 'response to phosphate starvation'. Pathways related to lipid and galactose metabolism were also enriched in the analyses indicating a species mechanism to deal with that deficiency. Genes associated with the synthesis of monogalactosyldiacylglycerol (MGDG), digalactosyldiacylglycerol (DGDG), and sulfoquinovosyldiacylglycerol (SQDG) were found over-expressed in plants grown in forest substrate. These compounds are galactolipids (MGDG and GDGD) and sulfolipids (SQDG) that constitute most of the chloroplast membrane lipids (15% are phospholipids), making the organelle minimally dependent on phosphate⁵⁸. During exposure to phosphorus deprivation, plants reallocate phosphate through the exchange of chloroplast membrane lipids^{59, 60}. The biosynthesis of galactolipids and sulfolipids is increased, replacing phospholipids and releasing phosphate to maintain nucleic acid levels and metabolic activity^{58, 59, 60}. Thus, *S. pulcherrimum* appears to have thrived on the forest substrate despite phosphate deficiency through the phosphorus reallocation from chloroplast membrane lipids and terpenoid precursors molecules.

Harsh environmental conditions limit the range of ecological strategies and lead to trait convergence. This convergence may or may not be the result of the expression of the same set of genes. Thus, we evaluated if the studied species show shared molecular strategies underlying adaptations to the substrates. The comparative ortholog transcriptomic analysis revealed that the expression patterns differed more between species than growth conditions, indicating that the overall gene expression pattern is organism-specific. Still, almost 300 pairs of orthologous genes in *P. platycephala* and *S. pulcherrimum* were observed with similar expression changes during development in *canga* and forest substrates. These transcripts code for proteins involved in the plant circadian rhythm. The circadian rhythm pathway and GO terms were also enriched in the species-specific analysis in the two conditions. The circadian rhythm is known to be synchronized by changes in light and temperature stimuli^{61, 62}. It allows plants to anticipate daily and seasonal changes in the environment essential to regulate their growth and survival⁶³. Several studies have demonstrated that the circadian clock contributes to the plants' ability to tolerate a wide spectrum of stress signals and acclimate to them, including iron deficiency, alkaline stress, and drought or salinity stress^{64, 65}. In this study, growth in *canga* soil down-regulated the

expression of *NIGHT LIGHT-INDUCIBLE AND CLOCK-REGULATED (LNKs 1, 2, and 3)*, *UNE10* (also known as *PIF8*), and *LATE ELONGATED HYPOCOTYL (LHY)*, expressed in the morning, while up-regulating evening-expressed genes (*PCL1*, *EARLY FLOWERING 4 - ELF4*, *PSEUDO-RESPONSE REGULATOR - PRR5*), and *CORs* (27 and 28) orthologs. The pattern of clock gene expression observed here seems to be related to the down-regulation of the chloroplast functions. Circadian regulation is integrated with photosynthesis, carbon fixation metabolism, and its metabolic products^{66, 67}. *CCA1*, an *Arabidopsis LHY* homologous, was found to increase activity in response to sugar. On the other hand, *PRR7* was found to be repressed⁶⁶. Indeed, pathways related to carbon metabolisms such as carbon fixation in photosynthetic organisms, glycolysis, and pentose phosphate pathways, were enriched in the down-regulated genes in both species in the species-specific analyses. Therefore, the substrate composition affected the expression of the circadian rhythm genes in the leaves, regulating the carbon fixation metabolism. This might provide adaptations to optimize plant performance in environments with different nutritional conditions.

Another possibility is that the studied plants altered the circadian clock phase by advancing the expression of evening-expressing genes, as the biological samples were collected in the morning. A similar advance of the circadian clock phase was also observed in barley under osmotic stress⁶⁸. The circadian clock has a role in micronutrient homeostasis regulation in plants, including acquisition and transport to the shoots^{69, 70, 71}. Chen and collaborators⁷¹ showed that Fe deficiency lengthened the circadian rhythm period in *Arabidopsis*. Both *P. platycephala* and *S. pulcherrimum* in the *canga* substrate exhibited high Fe concentration in the shoots¹⁴ that may be related to a shortened circadian period and explain the early expression of the evening genes. Observing the circadian rhythm genes expression at various time points during the day may elucidate if the *canga* substrate shortens the circadian period. Overall, many genes involved in the abiotic stress response are under the control of the circadian rhythm, even for environmental conditions that are constant in a diurnal manner, such as drought and salinity^{63, 65}. Our results suggest that plants adapted to both *canga* and forest environments can modulate the circadian rhythm in a substrate-dependent manner that might help them thrive in this range of conditions. The circadian clock is conserved among living species since it controls general metabolic processes and ensures plants' acclimation to their environment. One interesting possibility is investigating if *canga* endemic plants present diminished circadian rhythm plasticity, limiting their capacity to thrive in different environments. The modification of the circadian clock genes may enhance crop growth and yields^{72, 72}. Here we show that the modulation of circadian clock genes may improve local environment adaptation by nutritional status perception. Modification in these genes may also improve land rehabilitation.

Conclusion

The *canga* environment presents numerous plant stressors and, despite the harsh conditions, many plant species are well adapted and capable of thriving in this environment. In this study, we identified DEGs in two Fabaceae species, capable of inhabiting the forest and the *canga* environments, grown under contrasting substrate conditions, where they naturally occur. We observed that the substrate modulates

gene expression in *P. platycephala* and *S. pulcherrimum*. Both species exhibited changes in major metabolic pathways, such as biosynthesis of secondary metabolites and carbon metabolism, and adopted species-specific strategies for adaptation in the *canga* environment. Genes involved in plants' response to environmental stimuli, such as phenylpropanoid biosynthesis and photosynthesis, were altered in *P. platycephala*. *S. pulcherrimum* specific DEGs were associated with the phosphate deprivation response. Our results also show evidence that the studied species exhibit shared adaptative transcriptional responses to the *canga* environment. The modulation of circadian rhythm genes was a common mechanism related to the *canga* environment that forced a similar expression for each species.

Methods

Biological Material and experimental design

The leaf samples used in this research were obtained from the plant physiology study by Silva and collaborators (2018)¹⁴. In summary, *P. platycephala* and *S. pulcherrimum* were grown in four substrates collected from the Carajás Mineral Province, Pará, Brazil. The region is rich in iron ore deposits (with active mining activities). An area of *canga*, an adjacent forest, and two mine wastes soil substrates (Red waste and Yellow waste) were chosen for substrate collection. A detailed description of the site and soil types is available in Silva et al., 2018¹⁴.

Both species were grown in a greenhouse in trays of 35 cm x 24 cm x 18 cm (L x W x H) containing 12 L of the substrate. The temperature varied from 25 to 30°C, and the midday photosynthetic photon flux density (PPFD) was 1,500 $\mu\text{mol m}^{-2} \text{s}^{-1}$. Water availability was maintained at 70% of the soil water retention capacity by daily irrigation after trays weighting to determine water loss. After 45 days, leaf samples of two trays of each substrate were harvested for the RNA-seq experiment. All the samples were harvested during morning time (09:30-10:30 local time) to minimize the diurnal patterns among the samples.

RNA isolation, library preparation, and sequencing

Leaf samples under each condition were harvested, fast-frozen in liquid nitrogen, and then stored at -80 °C for posterior RNA extraction. The collected leaves from plants growing in the same tray were pooled together, ground in liquid nitrogen, and considered one compound replicate of each species. Each replicate consisted of leaves from three plants from the same tray. Total RNAs were extracted using the RNeasy mini kit (QIAGEN) following the manufacturer's protocols. RNA integrity and concentration were determined using a 2100 Bioanalyzer (Agilent Technologies, Waldbronn, Germany) and a Qubit® RNA High Sensitivity Assay Kit (Thermo Fisher Scientific, Waltham, MA, USA), respectively. Only RNAs with RIN (RNA Integrity Number) greater than 8 were used for the next steps. 100 ng of total RNA from each sample was used in the Ribo-Zero rRNA removal kit (Illumina, San Diego, CA). Subsequently, the rRNA-depleted RNA was processed using the TruSeq Stranded RNA library preparation kit (Illumina, San Diego, CA). The libraries were evaluated using Qubit® DNA Broad-range Assay Kit and 2100 Bioanalyzer.

Individual libraries were uniquely barcoded, multiplexed, and paired-end sequenced (2 x 150 bp) on the Illumina NextSeq 500 at the Instituto Tecnológico Vale, Belém, Pará, Brazil with the High Output kit (300 cycles). All raw reads generated from this study were deposited in the Short Read Archive (SRA) of NCBI under accession number PRJNA645405.

Transcriptome assembly

Raw reads were evaluated for quality using the fastQC program⁷⁴ and processed to filter Illumina adapters, and low-quality reads using Trimmomatic v. 0.38⁷⁵ with the following parameters: ILLUMINACLIP:TruSeq3-PE-2.fa:2:20:10 LEADING:3 TRAILING:3 SLIDINGWINDOW:5:20 MINLEN:35. Orphaned reads were assigned as single-end reads. The reads were also aligned to the Silva and RFAM databases to subtract rRNA reads that passed the rRNA depletion protocol. In order to produce the most accurate plants gene sets possible and to maximize the diversity and completeness of *de novo* assembled transcripts, the remaining clean reads were used to assemble transcripts with four different assemblers: Trinity v.2.8.3²⁰, with `-seqType fq -SS_lib_type RF -max_memory 260G` parameters; rnaSPAdes v. 3.12.0⁷⁶ with `-ss-rf` flag; Velvet v. 1.2.10/Oases v. 0.2.09²² with `-shortPaired -fastq -strand_specific` parameters for velvet, `-read_trkg yes` for velvetg and `-ins_length 100 -cov_cutoff auto` for oases; and SOAPDenovoTrans v. 1.03²¹ with `max_rd_len=150, rd_len_cutof=150, avg_ins=300, reverse_seq=0, asm_flags=3, map_len=32` parameters at the config file. Kmergenie v. 1.7039⁷⁷ was used to calculate the probable best k-mer size for assembling from the union of all libraries left reads, all right reads, and the union of all reads. Trinity was used with k-mer 25, rnaSPAdes was used with default parameters since it calculates internally the best k-mer size. Velvet/Oases and SOAPDenovo-Trans were used with multiple k-mers, ranging from 21 to 81 with a step size of 10 and the resulting k-mers from Kmergenie (*P. platycephala* – 31, 51 and 57; *S. pulcherrimum* – 27, 31 and 39). The cleaned paired-end reads were used for all assemblies, except for those generated with SOAPDenovo-Trans, which also included the cleaned single-end reads.

The resulting assemblies from each assembler were combined into one merged assembly for each species and processed to mitigate redundancy with the EvidentialGene tr2aacds v.4 pipeline¹⁹ (http://arthropods.eugenes.org/EvidentialGene/about/EvidentialGene_trassembly_pipe.html). The tr2aacds pipeline selects the best set of assembled transcripts from the input assembly based on coding potential. This pipeline uses several programs to 1) remove perfect redundancy (fastanrdb/exonerate-2.2.0), 2) remove perfect fragment (CD-HIT-EST), and 3) find high-identity exon-sized alignments (blastn) and output transcripts into three classes: okay (the best transcripts with the unique CDS), okalt (alternative transcripts, possible isoforms), and drop (the transcripts that did not pass the internal filter). Subsequently, this new program version does the second stage of analysis over the initial classes and reclassifies them into drop and okay. The okay set was selected for the subsequent analysis, including the main transcripts with alternates and those with no alternates.

As a measure of assembly accuracy, the percentage of correctly assembled bases was obtained by mapping Illumina reads back to the initial transcripts using Bowtie2 version 2.23⁷⁸. The completeness of

the assembled transcriptomes was assessed using BUSCO v.3.0.2²⁷ to obtain the percentage of single-copy orthologs represented in the embryophyta_odb9 and eudicotyledons_odb10 databases.

Annotation

The translated coding sequences produced from EvidentialGene were functionally annotated using the Trinotate v.3.2.1⁷⁹. Homology searches were performed against known proteins using BLASTp⁸⁰ against the UniProtKB/Swiss-Prot database, with an e-value of $1e10^{-6}$, and hmmer v.3.1b2 (<http://hmmer.org>) against the common protein domains of Pfam database⁸¹. Transmembrane regions were predicted using the tmhmm v.2⁸² server, and ribosomal RNA genes were detected with RNAMMER v.1.2⁸³. Annotation outputs were loaded into a Trinotate SQLite Database.

Assembly filtering

The Evigene draft transcripts sets for *P. platycephala* and *S. pulcherrimum* were filtered to discard possibly spurious loci. For this purpose, putative proteins shorter than 120aa long from the main set of transcripts were blasted (e-value 1×10^{-6}) against the UniProtKB/Swiss-Prot Viridiplantae database. The contigs codifying the short putative proteins with homology to the Viridiplantae database, the contigs codifying putative proteins longer than 120aa, and their alternative forms were used for differential expression (DE) analysis in each species.

Gene orthology prediction

The Orthofinder v. 2.3.12^{28,84} software was used to identify the two species' orthologous groups of protein sequences. Identification of orthogroups was conducted utilizing the Evigene predicted amino acid sequences after the above filtering step and classified as main or no class (i. e., not the alternate forms) since the authors recommend using a single representative transcript-variant for each gene in the analysis.

Further genome and transcriptome sequences of Caesalpinioideae were downloaded from various sources (See Supplementary Table 3, Additional File 1), including all the nuclear data used by Koenen and collaborators (2020)¹¹ and new sequences deposited at NCBI. The amino acid sequences were extracted from transcriptomes with EvidentialGene, and only the main set of transcripts were used as input for Orthofinder. The orthogroups of the 18 species used (including *P. platycephala* and *S. pulcherrimum*) were identified, and a species tree was constructed based on the Species Tree Inference from All Genes (STAG) method⁸⁵. STAG support values are calculated as the proportion of orthogroup trees that contain a bipartition out of the total number of orthogroup trees with at least one sequence (i. per species). MAFFT⁸⁶ was used to generate multiple sequence alignments and FastTree⁸⁷ to the gene trees.

Differential expression analysis

For each species, the number of transcripts expressed in plant growth in both *canga* and forest soil types was quantified by mapping each condition's cleaned reads to the respective filtered transcriptome

assembly using RSEM⁸⁸ and Bowtie2. We then calculated Spearman's correlation coefficients between all replicates using gene expression data. The DE analyses were performed using the estimated counts generated from RSEM with the edgeR package³⁵. *P*-values were corrected for multiple testing with the Benjamini and Hochberg procedure. A false discovery rate (FDR) cutoff value of 0.001 and a \log_2 FoldChange (\log_2 FC) of 2 were used to classify transcripts as differentially expressed in the species-specific analysis.

To the cross-species comparison, DE analysis was performed just with the orthologous genes shared between the two species obtained with Orthofinder, as proposed by Moreno-Santillán and collaborators (2019)⁸⁹. In brief, each biological replicate of each condition was aligned to its transcriptome with RSEM. The quantification files were edited to replace the transcript IDs generated by EvidentialGene, for its respective Single Gene Orthogroup name. The quantification files were concatenated to a single count matrix. To find orthogroups that behave similarly in plants under the different substrates, we performed DE analysis with the count matrix and the edgeR method using two-factor Generalized Linear Models (GLMs). The GLMs were implemented in edgeR using an additive model to correct the difference in gene expression between species, and obtain differentially expressed genes between conditions (design \downarrow model.matrix(~Species+Substrate)). *P*-values were corrected for multiple testing with the Benjamini and Hochberg procedure. glmTreat was used to classify orthologs as differentially expressed above Fold Change 2.

Gene Ontology (GO) enrichment analysis and Kyoto Encyclopedia of Gene and Genome (KEGG) pathway analysis were implemented by the Goseq R package³⁶ and KOBAS software³⁷, respectively, with *Medicago truncatula* as the background species for the KEGG analysis. GOs and pathways with FDR corrected *p*-value < 0.05 were considered significantly enriched. Significant GO annotations were processed with REVIGO⁹⁰ to summarize the main annotations and remove redundancy. The REVIGO output was then fed as input to CirGO⁹¹ for pie chart visualization. The GOChord function of the R package GOplot⁹² was also used to visualize the enriched GO terms in the DE orthologs. The R package ggplot2⁹³ was used for the enriched KEGG pathways visualization.

Declarations

Ethics approval and consent to participate

Seed lots from *P. platycephala* and *S. pulcherrimum* were obtained from Vale's tree nursery in Carajás, Pará, Brazil. The plant materials were identified by Lourival Tyski and Delmo Silva from Carajás herbarium (HCJS). The plants under this study are not rare or endangered. No specific permits were required for the sample collection. The research conducted complied with all institutional and national guidelines. The access to the Brazilian Genetic Heritage is registered in SisGen under the number A1FEDE4.

Consent for publication

Not applicable

Availability of data and materials

The raw datasets generated and analyzed during the current study are available in the NCBI Sequence Read Archive (SRA) repository under the Bioproject number PRJNA645405.

The datasets supporting the conclusions of this article are included in this article and its supplementary information files.

Competing interests

VALE SA supported the research at Instituto Tecnológico Vale (ITV). CC, MG, SR, and GO are VALE SA employees. MCD declares no competing interests. VALE SA did not influence the study design, data analysis, or the interpretation of the results.

Funding

This research was financially supported by VALE SA (444227/2018-0). VALE SA did not influence the study design, data analysis, or the interpretation of the results. The Brazilian National Council for Scientific and Technological Development (Conselho Nacional de Desenvolvimento Científico e Tecnológico - CNPq) supported M.C.D. (process number 381270/2018-1). GO is funded by CNPq (444227/2018-0, 402756/2018-5, 307479/2016-1) and the CABANA project (RCUK/BB/P027849/1).

Authors' contributions

The experimental design was previously determined by MG, CC, SR, and GO; MCD and MG collected samples; MCD conducted RNA extraction, library preparation, and sequencing. MCD performed the bioinformatics analysis on the RNA-seq data.; MCD wrote the manuscript with essential contributions from CC, MG, and GO; all authors revised and approved the final manuscript.

Acknowledgments

The authors would like to thank Dr. Simone Mitre and Dr. Joyce Silva for sample supply; Talvâne Lima, MSc. Renato Oliveira for help with scripts; Manoel João Pereira Lopes for technical support; Dr. Diego Sotero for the support in revising this work.

References

1. Posth NR, Konhauser KO, Kappler A. Banded Iron Formations. In: Reitner J, Thiel V, editors. Encyclopedia of Geobiology. Springer: Dordrecht, 2011. doi:10.1007/978-1-4020-9212-1_19.
2. Jacobi CM, Carmo FF, Vincent RC, Stehmann JR. Plant communities on the ironstone outcrops - a diverse and endangered Brazilian ecosystem. Biodivers. Conserv. 2007;16:2185–2200; doi:10.1007/s10531-007-9156-8.

3. Skirycz A, Castilho A, Chaparro C, Carvalho N, Tzotzos G, Siqueira JO. Canga biodiversity, a matter of mining. *Front. Plant Sci.* 2014;5:1–9.
4. Mitre SK, Mardegan SF, Caldeira CF, Ramos SJ, Furtini Neto AE, Siqueira JO, Gastauer M. Nutrient and water dynamics of Amazonian *canga* vegetation differ among physiognomies and from those of other neotropical ecosystems. *Plant Ecol.* 2018;219:1341–1353; doi:10.1007/s11258-018-0883-6.
5. Nunes JA, Schaefer CEGR, Ferreira Júnior WG, Neri AV, Correa GR, Enright NJ. Soil-vegetation relationships on a banded ironstone 'island', Carajás Plateau, Brazilian Eastern Amazonia. *Anais da Academia Brasileira de Ciências.* 2015;87(4):2097–2110; doi:10.1590/0001-376520152014-0106.
6. Giulietti AM, Pirani JR, Harley RM. Espinhaço Range region, eastern Brazil. In: Davis SD, Heywood VH, Herrera-Macbride O, Villa-Lobos J, Hamilton AC (eds) *Centres of plant diversity: a guide and strategy for their conservation.* IUCN Publication Unit, Cambridge, 1997; 397–404.
7. SILVA MFF. Distribuição de metais pesados na vegetação metalófica de Carajás. *Acta Bot. Bras.* 1992; 6:107–22.
8. Mattos CMJ, Silva WLS, Carvalho CS, Lima AN, Faria SM, Lima HC. Flora das cangas da serra dos Carajás, Pará, Brasil: Leguminosae. *Rodriguésia.* 2018;69(3):1147–1220.
9. LPWG (Legume Phylogeny Working Group). A new subfamily classification of the Leguminosae based on a taxonomically comprehensive phylogeny. *Taxon.* 2017;66:44–77.
10. Tedersoo L, Laanisto L, Rahimlou S, Toussaint A, Hallikma T, Pärtel M. Global database of plants with root-symbiotic nitrogen fixation: NodDB. *Journal of Vegetation Science.* 2018;29(3):560–568; doi:10.1111/jvs.12627.
11. Koenen EJM, Ojeda DI, Steeves R, Migliore J, Bakker FT, Wieringa, JJ, Kidner C, Hardy OJ, Pennington RT, Bruneau A, Hughes CE. Large-scale genomic sequence data resolve the deepest divergences in the legume phylogeny and support a near-simultaneous evolutionary origin of all six subfamilies. *New Phytol.* 2020;225(3):1355–1369.
12. Forzza RC, Baumgratz JFA, Bicudo CEM, Carvalho Jr AA, Costa A, Costa DP. *Catálogo de plantas e fungos do Brasil.* Rio de Janeiro: Andrea Jakobsson Estúdio - Instituto de Pesquisa Jardim Botânico do Rio de Janeiro, 2010; 828 p. Vol. 2. ISBN 978-85-8874-243-7. Available from SciELO Books <<http://books.scielo.org>>.
13. Giannini TC, Giulietti AM, Harley RM, *et al.* Selecting plant species for practical restoration of degraded lands using a multiple-trait approach. *Austral Ecology.* 2016; doi:10.1111/aec.12470.
14. Silva JS, Gastauer M, Ramos SJ, Mitre S, Neto AEF, Siqueira O, Caldeira CF. Initial growth of Fabaceae species: Combined effects of topsoil and fertilizer application for mineland revegetation. *Flora.* 2018;246 doi:10.1016/j.flora.2018.08.001.
15. Ramos SJ, Caldeira CF, Gastauer M, Costa DLP, Furtini Neto AE, Souza FBM, Souza-Filho PWM, Siqueira JO. Native leguminous plants for mineland revegetation in the eastern Amazon: seed characteristics and germination. *New Forests.* 2019;50:859–872; doi:10.1007/s11056-019-09704-1.
16. Gastauer M, Sarmento PSM, Santos VCA, Caldeira CF, Ramos SJ, Teodoro GS, Siqueira JO. Vegetative functional traits guide plant species selection for initial mineland rehabilitation.

- Ecological Engineering. 2020;148; doi:10.1016/j.ecoleng.2020.105763.
17. Lorenzi H. Árvores brasileiras: manual de identificação e cultivo de plantas arbóreas nativas do Brasil. São Paulo: Instituto Plantarum. 2002;2:179–187.
 18. Ntiamao-Baidu Y. Can wildlife contribute to food security in Africa? Issues and conclusions. In: Ntiamao-Baidu editor. Wildlife and food security in Africa. 1997;91-99; ISBN 92-5-104103-2 (FAO of the United Nations).
 19. Gilbert D. Gene-omes built from mRNA seq not genome DNA. 7th annual arthropod genomics symposium. Notre Dame. 2013.
<http://arthropods.eugenes.org/EvidentialGene/about/EvigeneRNA2013poster.pdf>
doi:10.7490/f1000research.1112594.1.
 20. Grabherr MG., Haas BJ, Yassour M, *et al.* Full-length transcriptome assembly from RNA-Seq data without a reference genome. *Nature Biotechnology* 2011;29(7):644–652; doi:10.1038/nbt.1883.
 21. Xie Y, Wu G, Tang J, *et al.* SOAPdenovo-Trans: De novo transcriptome assembly with short RNA-Seq reads. *Bioinformatics*. 2013;30(12):1660–1666. doi:10.1093/bioinformatics/btu077.
 22. Schulz, M. H., Zerbino D. R., Vingron M, Birney E. Oases: Robust de novo RNA-seq assembly across the dynamic range of expression levels. *Bioinformatics*. 2012;28(8):1086–1092; doi:10.1093/bioinformatics/bts094.
 23. Torales SL, Rivarola M, Pomponio MF, *et al.* De novo assembly and characterization of leaf transcriptome for the development of functional molecular markers of the extremophile multipurpose tree species *Prosopis alba*. *BMC Genomics*. 2013;14:705; doi:10.1186/1471-2164-14-705.
 24. Gilbert D. Longest protein, longest transcript or most expression, for accurate gene reconstruction of transcriptomes? Preprint at bioRxiv 829184. 2019; doi:10.1101/829184.
 25. Hsieh PH, Oyang YJ, Chen CY. Effect of de novo transcriptome assembly on transcript quantification. *Sci. Rep.* 2019;9:8304; doi:10.1038/s41598-019-44499-3.
 26. Spillane JL, LaPolice TM, MacManes, MD, Plachetzki DC, Signal, bias, and the role of transcriptome assembly quality in phylogenomic inference. Preprint at bioRxiv. 2020; doi:10.1101/2020.07.23.216606.
 27. Simão FA, Waterhouse RM, Ioannidis P, Kriventseva EV, Zdobnov EM BUSCO: Assessing genome assembly and annotation completeness with single-copy orthologs. *Bioinformatics* 2015;31:3210–3212.
 28. Emms DM, Kelly S. OrthoFinder: solving fundamental biases in whole genome comparisons dramatically improves orthogroup inference accuracy. *Genome Biology*. 2015;16:157.
 29. Emms DM, Kelly S. STRIDE: Species Tree Root Inference from Gene Duplication Events. *Molecular Biology and Evolution*. 2017;34(12):3267–3278. doi:10.1093/molbev/msx259.
 30. Oliveira LC. Filogenia de *Parkia* R.Br. (Leguminosae: Mimosoideae) baseada em sequências de DNA de cloroplasto. Instituto Nacional Pesquisas da Amazônia – INPA. 2015.

31. Simon MF, Pastore JFB, Souza AF, Borges LM, Scalon V, Ribeiro PG, Silva JS, Souza V, Queiroz L. Molecular phylogeny of *Stryphnodendron* (Mimosoideae, Leguminosae) and generic delimitations in the *Piptadenia* group. *International Journal of Plant Sciences* 2016;177:44–59.
32. Wang YH, Qu XJ, Chen SY, Li DZ, Yi TS. Plastomes of Mimosoideae: structural and size variation, sequence divergence, and phylogenetic implication. *Tree Genetics & Genomes*. 2017;13:41.
33. Assefa AT, Vandesompele J, Thas O. On the utility of RNA sample pooling to optimize cost and statistical power in RNA sequencing experiments. *BMC Genomics* 2020; 21:312. doi:10.1186/s12864-020-6721-y.
34. Schurch NJ, Schofield P, Gierliński M, et al. How many biological replicates are needed in an RNA-seq experiment and which differential expression tool should you use? *RNA*. 2016;22(6):839–851. doi:10.1261/rna.053959.115
35. Robinson MD, McCarthy DJ, Smyth GK. EdgeR: A Bioconductor Package for Differential Expression Analysis of Digital Gene Expression Data. *Bioinformatics*. 2010;26(1):139–40.
36. Young MD, Wakefield MJ, Smyth GK, Oshlack A. Gene ontology analysis for RNA-seq: accounting for selection bias. *Genome Biol*. 2010;11(2):14.
37. Mao X, Cai T, Olyarchuk JG, Wei L. Automated genome annotation and pathway identification using the KEGG Orthology (KO) as a controlled vocabulary. *Bioinformatics*. 2005;21(19):3787–3793.
38. Guevara DR, Champigny MJ, Tattersall A, et al. Transcriptomic and metabolomic analysis of Yukon *Thellungiella* plants grown in cabinets and their natural habitat show phenotypic plasticity. *BMC plant biology* 2012;12:175; doi:10.1186/1471-2229-12-175.
39. Sinha R, Gupta A, Senthil-Kumar M. Concurrent Drought Stress and Vascular Pathogen Infection Induce Common and Distinct Transcriptomic Responses in Chickpea. *Front. Plant Sci*. 2017; doi: 10.3389/fpls.2017.00333.
40. Fajardo-Cavazos P, Morrison MD, Miller KM, Schuerger AC, Nicholson WL. Transcriptomic responses of *Serratia liquefaciens* cells grown under simulated Martian conditions of low temperature, low pressure, and CO₂-enriched anoxic atmosphere. *Sci Rep*. 2018;8(1):14938; doi:10.1038/s41598-018-33140-4.
41. Cho SM, Lee H, Jo H, Lee H, Kang Y, Park H, Lee J. Comparative transcriptome analysis of field- and chamber-grown samples of *Colobanthis quitensis* (Kunth) Bartl, an Antarctic flowering plant. *Sci Rep* 2018;8:11049; doi:10.1038/s41598-018-29335-4.
42. Isah T. Stress and defense responses in plant secondary metabolites production. *Biol. Res*. 2019;52(1):39; doi:10.1186/s40659-019-0246-3.
43. Jan R, Asaf S, Numan M, Lubna, Kim K-M. Plant Secondary Metabolite Biosynthesis and Transcriptional Regulation in Response to Biotic and Abiotic Stress Conditions. *Agronomy*. 2021; 11(5):968; doi:10.3390/agronomy11050968
44. Liu Q, Luo L, Zheng L. Lignins: Biosynthesis and Biological Functions in Plants. *Int. J. Mol. Sci*. 2018;19:335.

45. Diaz J, Bernal A, Pomar F, Merino F. Induction of shikimate dehydrogenase and peroxidase in pepper (*Capsicum annuum* L.) seedlings in response to copper stress and its relation to lignification. *Plant Sci.* 2001;161:179–188.
46. Gao L, Peng K, Chen Y, Wang G, Shen Z. Roles of apoplastic peroxidases, laccases, and lignification in the manganese tolerance of hyperaccumulator *Phytolacca americana*. *Acta Physiol. Plant* 2012;34:151–159.
47. Bhardwaj R, Handa N, Sharma R, Kaur H, Kohli S, Kumar V, Kaur P. Lignins and abiotic stress: An overview. In: Ahmad P, Wani M, editors. *Physiological Mechanisms and Adaptation Strategies in Plants Under Changing Environment*. Springer: New York. 2014; doi:10.1007/978-1-4614-8591-9_10.
48. Yang S, Yi K, Chang MM, Ling GZ, Zhao ZK, Li XF. Sequestration of Mn into the cell wall contributes to Mn tolerance in sugarcane (*Saccharum officinarum* L.). *Plant Soil* 2019;436:475–487.
49. Kim YH, Huh GH. Overexpression of cinnamyl alcohol dehydrogenase gene from sweetpotato enhances oxidative stress tolerance in transgenic Arabidopsis. *In Vitro Cell.Dev.Biol.-Plant* 2019;55:172–179; doi:10.1007/s11627-018-09951-5.
50. Kapoor D, Singh S, Kumar V, Romero R, Prasad R, Singh J. Antioxidant enzymes regulation in plants in reference to reactive oxygen species (ROS) and reactive nitrogen species (RNS). *Plant Gene* 2019;19; doi:10.1016/j.plgene.2019.100182.
51. Brestic M, Zivcak M, Kunderlikova K, Allakhverdiev SI. High temperature specifically affects the photoprotective responses of chlorophyll b-deficient wheat mutant lines. *Photosynth. Res.* 2016;130:251–266.
52. Tahmasebi A, Ashrafi-Dehkordi E, Shahriari AG, Mazloomi SM, Ebrahimie E. Integrative meta-analysis of transcriptomic responses to abiotic stress in cotton. *Progress in Biophysics and Molecular Biology* 2019;146:112–122.
53. Cohen SP, Leach JE. Abiotic and biotic stresses induce a core transcriptome response in rice. *Sci. Rep.* 2019;9:6273; doi:10.1038/s41598-019-42731-8.
54. Paunov M, Koleva L, Vassilev A, Vangronsveld J, Goltsev V. Effects of different metals on photosynthesis: cadmium and zinc affect chlorophyll fluorescence in durum wheat. *Int. J. Mol. Sci.* 2018;19(3):787.
55. Cheng A, Lou Y, Mao Y, Lu S, Wang L, Chen X. Plant terpenoids: Biosynthesis and ecological functions. *J. Integr. Plant. Biol.* 2007, 49:179–186; doi:10.1111/j.1744-7909.2007.00395.x.
56. Ormeño E, Fernandez C. Effect of Soil Nutrient on Production and Diversity of Volatile Terpenoids from Plants. *Curr Bioact Compd.* 2012; 8(1):71–79; doi:10.2174/157340712799828188
57. Bustamante MÁ, Michelozzi M, Barra Caracciolo A, et al. Effects of Soil Fertilization on Terpenoids and Other Carbon-Based Secondary Metabolites in *Rosmarinus officinalis* Plants: A Comparative Study. *Plants (Basel)*. 2020;9(7):830; doi:10.3390/plants9070830
58. Cook R, Lupette J, Benning C. The Role of Chloroplast Membrane Lipid Metabolism in Plant Environmental Responses. *Cells* 2021, 10:706; doi:10.3390/cells10030706

59. Yu B, Xu C, Benning C. Arabidopsis disrupted in SQD2 encoding sulfolipid synthase is impaired in phosphate-limited growth. *Proceedings of the National Academy of Sciences of the United States of America*. 2002; 99(8):5732–5737. doi: 10.1073/pnas.082696499
60. Kobayashi K, Awai K, Nakamura M, Nagatani A, Masuda T, Ohta H. Type-B monogalactosyldiacylglycerol synthases are involved in phosphate starvation-induced lipid remodeling, and are crucial for low-phosphate adaptation. *Plant J*. 2009;57:322–331.
61. Dodd AN, Salathia N, Hall A, Kévei E, Tóth R, Nagy F, Hibberd JM, Millar AJ, Webb AA. Plant Circadian Clocks Increase Photosynthesis, Growth, Survival, and Competitive Advantage. *Science* 2005;309(5734):630–633; doi:10.1126/science.1115581.
62. Yerushalmi S, Green RM. Evidence for the adaptive significance of circadian rhythms. *Ecology Letters* 2009;12(9):970–981.
63. Caldeira CF, Jeanguenin L, Chaumont F, Tardieu F. Circadian rhythms of hydraulic conductance and growth are enhanced by drought and improve plant performance. *Nat Commun*. 2014;5:5365; doi:10.1038/ncomms6365.
64. Li M, Cao L, Mwimba M, Zhou Y, Li L, Zhou M, Schnable PS, O'Rourke JA, Dong X, Wang W. Comprehensive mapping of abiotic stress inputs into the soybean circadian clock. *PNAS*. 2019;116(47):23840–23849; doi:10.1073/pnas.1708508116.
65. Grundy J, Stoker C, Carré IA. Circadian regulation of abiotic stress tolerance in plants. *Front Plant Sci*. 2015;6:648; doi:10.3389/fpls.2015.00648.
66. Haydon MJ, Mielczarek O, Robertson FC, Hubbard KE, Webb AA. Photosynthetic entrainment of the Arabidopsis thaliana circadian clock. *Nature*. 2013;502(7473):689–692. doi:10.1038/nature12603
67. Dodd AN, Belbin FE, Frank A, Webb AA. Interactions between circadian clocks and photosynthesis for the temporal and spatial coordination of metabolism. *Front Plant Sci*. 2015;6:245. doi:10.3389/fpls.2015.00245
68. Habte E, Müller LM, Shtaya M, Davis SJ, von Korff M. Osmotic stress at the barley root affects expression of circadian clock genes in the shoot. *Plant Cell Environ*. 2014;37(6):1321–7. doi:10.1111/pce.12242.
69. Perea-García A, Andrés-Colás N, Peñarrubia L. Copper homeostasis influences the circadian clock in Arabidopsis. *Plant signaling & behavior*. 2010;5(10):1237–1240; doi:10.4161/psb.5.10.12920
70. Haydon MJ, Bell LJ, Webb AA. Interactions between plant circadian clocks and solute transport. *J. Exp. Bot*. 2011;62:2333–2348.
71. Chen YY, Wang Y, Shin LJ, Wu JF, Shanmugam V, Tsednee M, Lo JC, Chen CC, Wu SH, Yeh KC. Iron is involved in the maintenance of circadian period length in Arabidopsis. *Plant physiology*, 2013;161(3):1409–1420; doi:10.1104/pp.112.212068.
72. Li M-W, Lam H-M. The Modification of Circadian Clock Components in Soybean During Domestication and Improvement. *Front. Genet.*, 2020; 11:571188; doi: 10.3389/fgene.2020.571188
73. Steed G, Ramirez DC, Hannah MA, Webb AAR. Chronoculture, harnessing the circadian clock to improve crop yield and sustainability. *Science*, 2021;372, eabc9141. doi: 10.1126/science.abc9141.

74. Andrews S. FastQC: A quality control tool for high throughput sequence data. 2010. <http://www.Bioinformatics.Babraham.Ac.UK/Projects/Fastqc/>, <http://www.bioinformatics.babraham.ac.uk/projects/>
75. Bolger AM, Lohse M, Usadel B Trimmomatic: a flexible trimmer for Illumina sequence data. *Bioinformatics* 2014;30:2114–2120.
76. Bankevich A, Nurk S, Antipov D, *et al.* SPAdes: a new genome assembly algorithm and its applications to single-cell sequencing. *Journal of Computational Biology* 2012;19(5):455–477; doi:10.1089/cmb.2012.0021.
77. Chikhi R, Medvedev P. Informed and Automated k-Mer Size Selection for Genome Assembly. *Bioinformatics* 2014;30(1):31–7.
78. Langmead B, Salzberg S. Fast gapped-read alignment with Bowtie 2. *Nature Methods*. 2012;9:357–359.
79. Bryant DM, Johnson K, DiTommaso T, *et al.* (2017) A tissue-mapped axolotl de novo transcriptome enables identification of limb regeneration factors. *Cell reports* 2017;18(3):762-776; doi:10.1016/j.celrep.2016.12.063.
80. Altschul SF, Gish W, Miller W, Myers EW, Lipman DJ. Basic local alignment search tool. *Journal of Molecular Biology* 1990;215(3):403–410
81. El-Gebali S, Mistry J, Bateman A, *et al.* The Pfam protein families database in 2019, *Nucleic Acids Research*. 2019;47(D1):D427–D432. doi:10.1093/nar/gky995
82. Krogh A, Larsson B, von Heijne G, Sonnhammer EL. Predicting Transmembrane Protein Topology with a Hidden Markov Model: Application to Complete Genomes. *J. Mol. Biol.* 2001;305:567–580.
83. Lagesen K, Hallin P, Rødland EA, Staerfeldt HH, Rognes T, Ussery DW. RNAmmer: consistent and rapid annotation of ribosomal RNA genes. *Nucleic acids research*, 2007;35(9):3100–3108.
84. Emms D, Kelly S. OrthoFinder: phylogenetic orthology inference for comparative genomics. *Genome Biology* 2019;20:238.
85. Emms D, Kell S. STAG: Species Tree Inference from All Genes. Preprint at bioRxiv. 2018. doi:10.1101/267914.
86. Benning C. MAFFT - a multiple sequence alignment program. *Annual Review of Cell and Developmental Biology* 2009;25:71–91.
87. Price MN, Dehal PS, Arkin AP Fasttree: Computing large minimum evolution trees with profiles instead of a distance matrix. *Mol. Biol. Evol.* 2009;26:1641–1650.
88. Li B, Dewey CN. RSEM: Accurate transcript quantification from RNA-seq data with or without a reference genome. *BMC Bioinformatics* 2011;12:323.
89. Moreno-Santillán DD, Machain-Williams C, Hernández-Montes G, Ortega J. De Novo Transcriptome Assembly and Functional Annotation in Five Species of Bats. *Sci. Rep.* 2019;9:6222; doi:10.1038/s41598-019-42560-9

90. Supek F, Bošnjak M, Škunca N, Šmuc T. REVIGO summarizes and visualizes long lists of Gene Ontology terms. PLOS ONE 2011;6(7): e21800; doi:10.1371/journal.pone.0021800
91. Kuznetsova I, Lugmayr A, Siira SJ, Racham O, Filipovska A. CirGO: an alternative circular way of visualising gene ontology terms. BMC Bioinformatics 2019;20:84. doi:10.1186/s12859-019-2671-2
92. Walter W, Sánchez-Cabo F, Ricote M. GOplot: an R package for visually combining expression data with functional analysis. Bioinformatics 2015;31(17):2912–4. doi:10.1093/bioinformatics/btv300
93. Wickham H. ggplot2: Elegant Graphics for Data Analysis. Springer-Verlag New York. ISBN 978-3-319-24277-4. 2016. <https://ggplot2.tidyverse.org>.

Figures

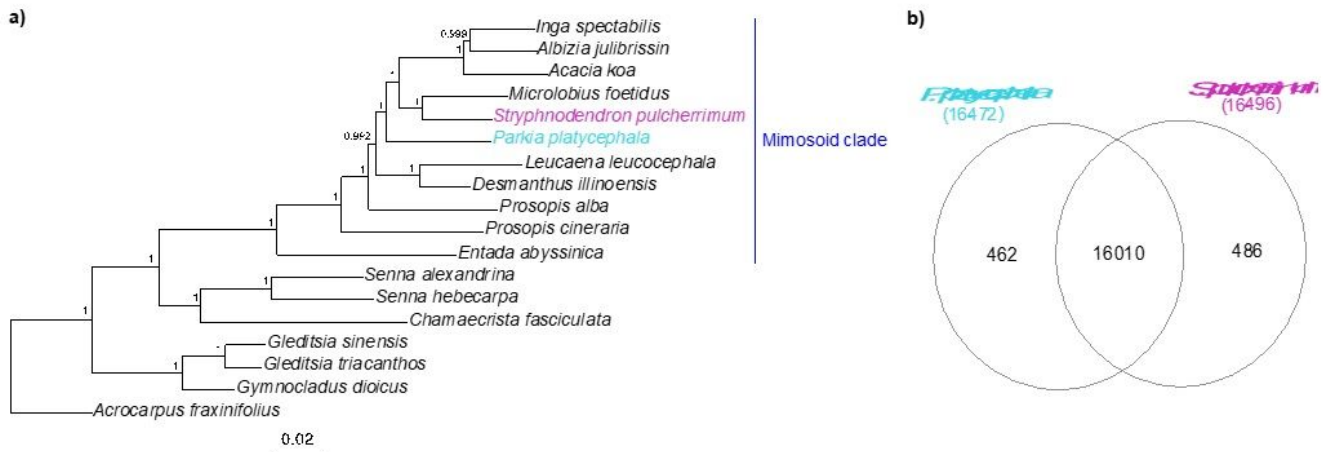


Figure 1

(a) Approximate Maximum Likelihood phylogenetic tree based in single-copy orthologs of Caesalpinioideae species, generated with OrthoFinder. The branch points' numbers represent support values based on 1,000 local bootstrapping resamples generated with FastTree. (b) Venn diagram illustrating the number of species-specific and overlapping protein orthogroups between the two plant transcriptome assemblies. The number of orthogroups was identified with OrthoFinder.

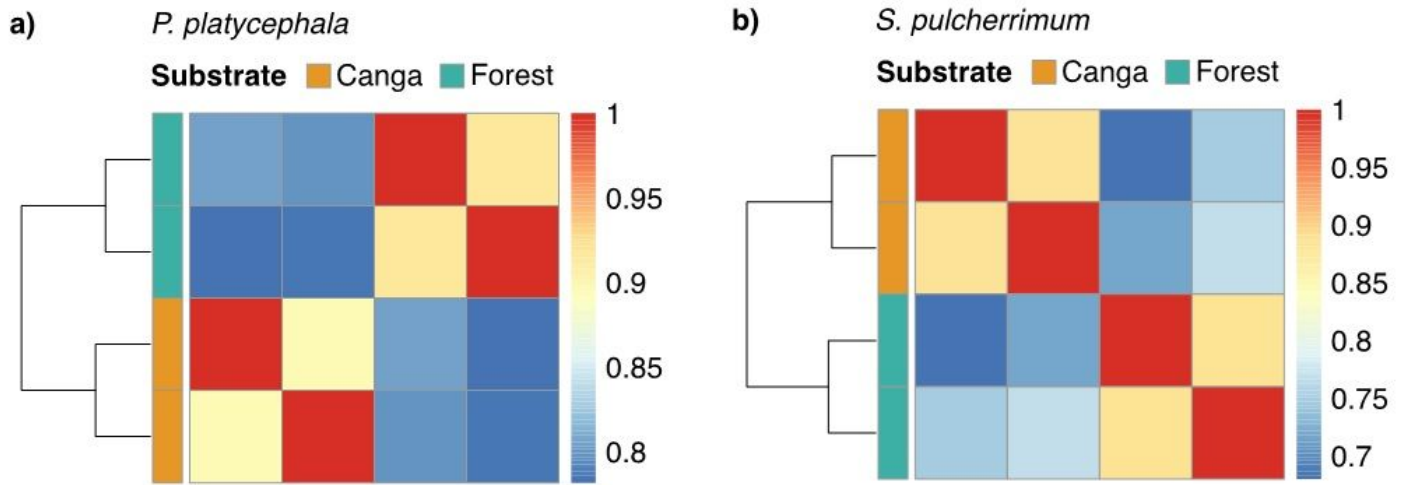


Figure 2

Sample clustering and correlation analysis. (a) Symmetrical heat map showing the Spearman's correlation coefficients of gene expression across the samples for *P. platycephala*. (b) Symmetrical heat map showing the Spearman's correlation coefficients of gene expression across the samples for *S. pulcherrimum*. Correlation coefficients are shown on the left ranging from blue (low similarity) to red (high similarity).

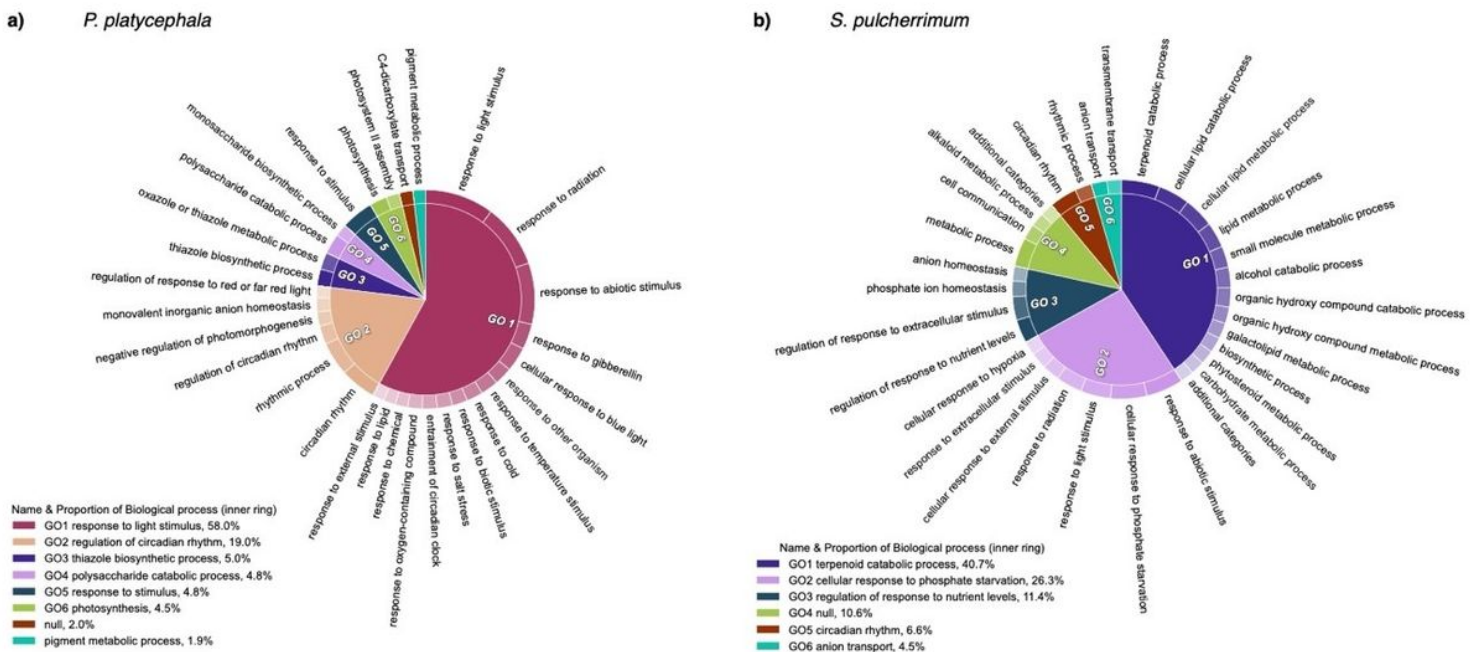


Figure 3

Enriched biological processes among DEGs between plants grown in canga and forest substrates. CirGO visualization of the top 30 GO enriched biological processes (FDR < 0.05) in a two-level hierarchical structure from the DEGs of (a) *P. platycephala* and (b) *S. pulcherrimum*. The legend shows the "parent"

labels, represented in the pie chart's inner ring and the slice proportion. The outer ring of the pie chart represents the relative contribution of "child" labels.

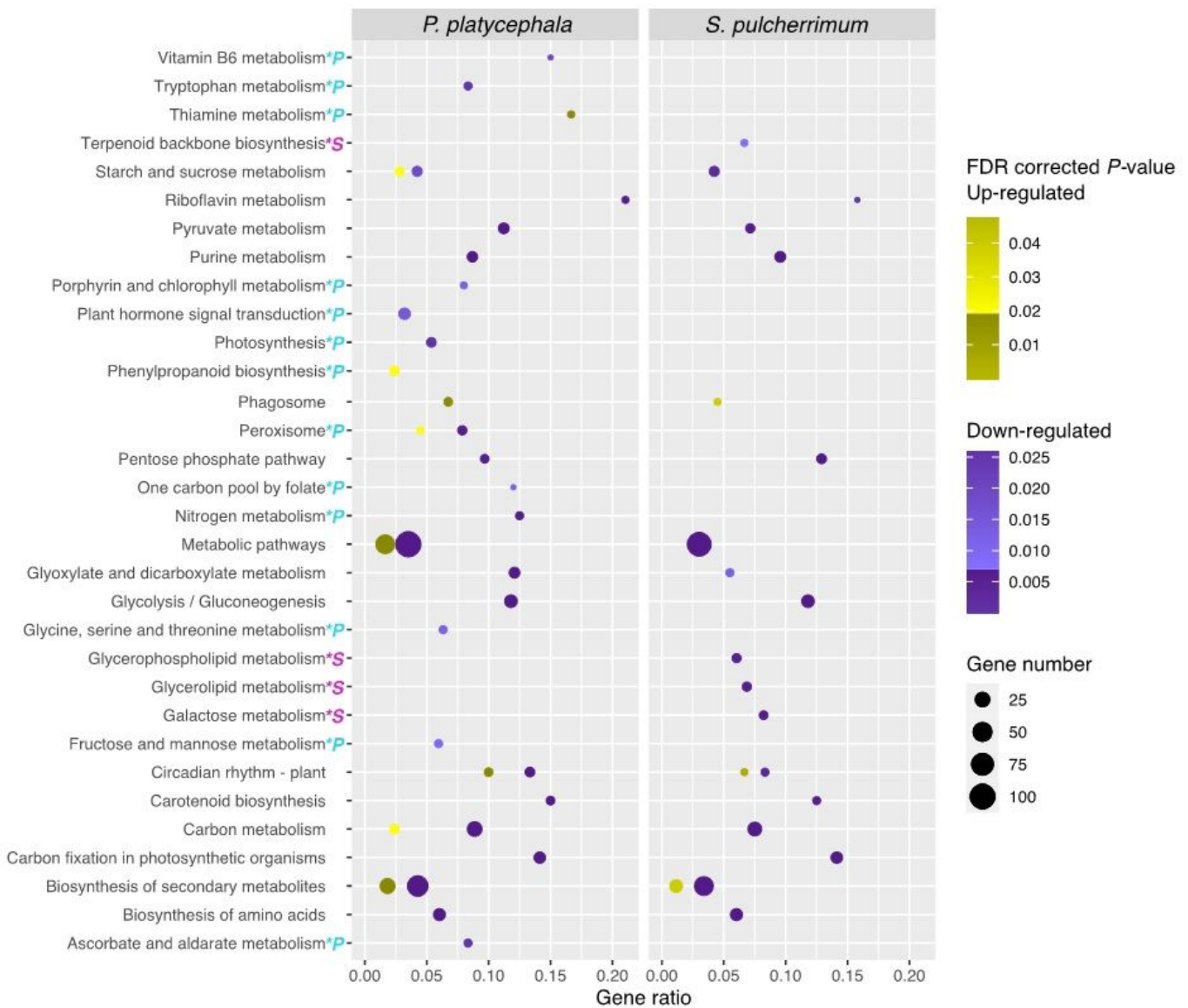


Figure 4

Enriched KEGG pathways among DEGs between plants grown in canga and forest substrates. Scatterplots of enriched KEGG pathways in up-regulated (yellow shades) and down-regulated (purple shades) gene groups for *P. platycephala* (left) and *S. pulcherrimum* (right). The significantly enriched pathways were indicated as dots (FDR < 0.05), and the dot sizes represent the number of the genes included in each cluster. The x-axis represents the ratio of the number of differentially expressed genes and all genes in the pathway. The deeper the color, the smaller the FDR corrected p-value. Colored letters next to the names of the routes indicate uniquely altered pathways in one species. P in cyan - *P. platycephala*; S in pink - *S. pulcherrimum*.

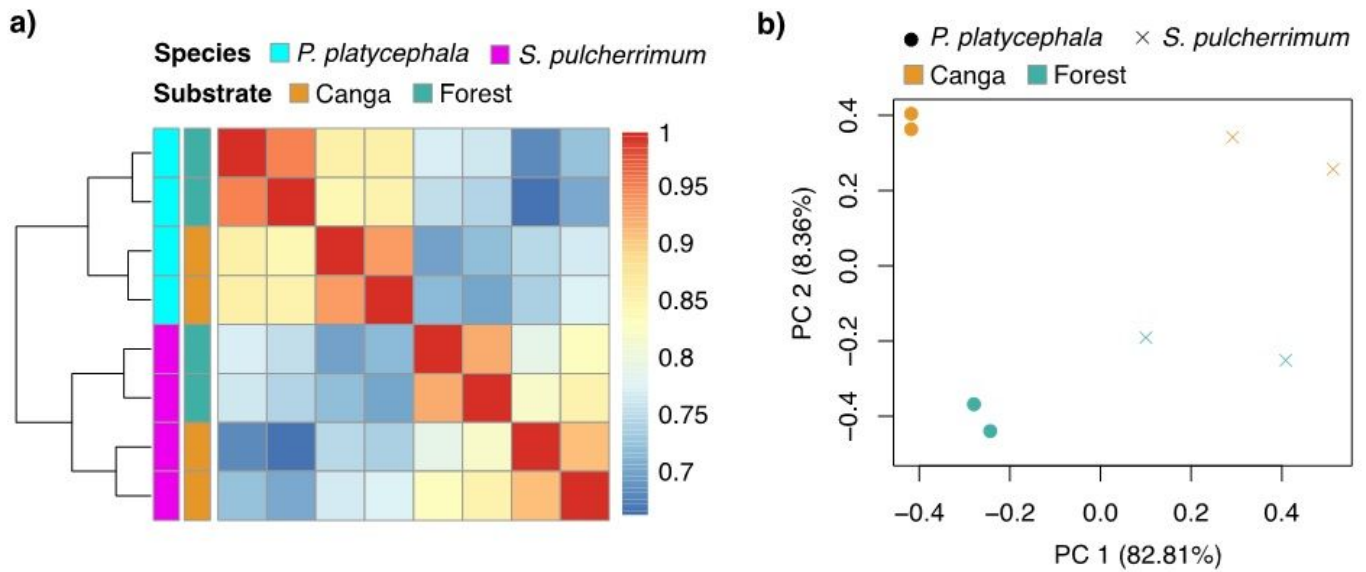


Figure 5

Cross-substrates comparison of ortholog expression patterns. (a) Symmetrical heat map of Spearman's correlation coefficients between all samples across all single-copy orthologs. Correlation coefficients are shown on the left ranging from blue (low similarity) to red (high similarity) (b) PCA of the log-transformed normalized expression levels of the single-copy orthologs between the two species grown in the canga and forest substrates. Species are represented by point shape; substrates are represented by point color.

Supplementary Files

This is a list of supplementary files associated with this preprint. Click to download.

- [Additionalfile1.xlsx](#)